Structural rationale for the chiral separation and migration order reversal of clenpenterol enantiomers in capillary electrophoresis using β-cyclodextrins

Antonio Salgado,[a*] Elene Tatunashvili,[b] Ann Gogolashvili,[b] Bezhan Chankvetadze,[b] and Federico Gago[c]

[a] *NMR Spectroscopy Centre (CERMN), CAI Químicas, Faculty of Pharmacy, University of Alcalá, E-28805 Alcalá de Henares, Madrid, Spain.*
[b] *Institute of Physical and Analytical Chemistry, School of Exact and Natural Sciences, Tbilisi State University, 0179 Tbilisi, Georgia.*
[c] *Department of Biomedical Sciences (Unidad Asociada IQM-CSIC) and Instituto de Investigación Química "Andrés M. del Río" (IQAR), University of Alcalá, E-28805 Alcalá de Henares, Madrid, Spain.*

Electronic Supplementary Information

Materials and methods

Reagents and analytes. Racemic clenpenterol (CPT) and β-cyclodextrin (βCD) were acquired from Sigma-Aldrich (Steinheim, Germany). Heptakis(2,3-di-O-acetyl)-β-cyclodextrin (HDA-βCD) was synthesized according to a published method.[1] Briefly, the primary hydroxyl groups in βCD were protected with *tert*-butylchlorodimethylsilane, and followed by treatment with acetic anhydride to acetylate the unprotected hydroxyl groups at positions 2 and 3. The protecting *tert*-butyldimethylsilyl groups were then removed by treatment with boron trifluoride etherate solution. Water was of Milli-Q quality (Millipore, Bedford, MA, USA). Deuterium oxide (99.9% deuterium), phosphoric acid-d_3 (D_3PO_4) solution in D_2O, (85% w/w, 98% atom D) and sodium deuteroxide (NaOD) solution in D_2O (40% wt) were from Sigma (St. Louis, MO, USA). All CE experiments were carried out on a capillary electrophoresis system Agilent G1600 (Agilent Technologies, Waldbronn, Germany) equipped with an autosampler, an on-column diode-array detector and air-based temperature control system. The Chemstation B.04.03 software from Agilent Technologies was used for instrument control and data analysis. Fused-silica capillaries were provided by Polymicro Technologies (Phoenix, AZ, USA).

Enantioseparation of racemic CPT by CE was performed in 50 mM potassium dihydrogenphosphate buffer at pH 2.0. Experimental conditions were as follows: uncoated fused-silica capillary, 50 μm ID x 43 (50) cm effective and total lengths, respectively. The samples were injected by pressure (10-13 mbar) for 3 s, the experiments were performed under constant voltage 10-25 kV, the separation temperature was set to 20°C and the detection wavelengths at 200 and 220 nm. Before each injection, the capillary was washed with 1N NaOH for 2 min, then BGE for another 2 min and finally with BGE containing the chiral selector for another 1 minute. At the end of each working day, the capillary was rinsed for 30 min with 0.1M NaOH, 30 min with the BGE and 15 min with water. Capillary wash cycles were performed at a pressure of approximately 1 bar.

NMR spectroscopy. All NMR experiments were run in a Varian 500 INNOVA NMR system (Palo Alto, CA, USA), fitted with an inverse 5 mm HCX 500 MHz probe head, a variable temperature controller and a z-gradient unit. The operating ^{1}H frequency of the spectrometer was 499.61 MHz. The ^{1}H 90^o hard pulse width was optimized for each sample. The ^{1}H spectral width was set to 8012.8 Hz. All NMR signals were assigned based on COSY, TOCSY and HSQC data, when appropriate. For the 1D ROESY experiments, all excitation windows were manually selected (depending on the comparative isolation of the spin system to study), with which the duration and potency of the soft (selective) excitation pulses were automatically adjusted with the VnmrJ

software (version 3.2 revision A). The number of transients in each 1D ROESY experiment was set to 512. The duration of the low power pulse for mixing was 400 ms. All NMR experiments were run at 25 °C. All NMR spectra were processed with the Mestre NOVA software (version 11.0.2, Mestrelab Research S. L., Santiago de Compostela, Spain). The concentration of the analytes in the NMR samples was about 30-fold higher than in the CE experiments so that reproducible NMR spectra were obtained. The solvent was 50 mM D_3PO_4 in D_2O, adjusted to an apparent pH 2 with sodium deuteroxide in D_2O (40% wt). Mixtures of racemic CPT (3.1 mg) and βCD (12.0 mg), and racemic CPT (2.7 mg) and HDA-βCD (14.0 mg), were each dissolved in 0.7 mL solvent. All samples were vortexed for 1 min and filtered through 0.45 μm polypropylene filters prior to data acquisition.

Separation of CPT enantiomers by high-performance liquid chromatography. CPT enantiomers were separated by HPLC using a Lux Cellulose-3 column (4.6 mm x 250 mm with 5-μm particles, Phenomenex, Torrance, CA, USA) thermostated at 25 °C. Methanol/water/diethylamine (65:35:0.1, v/v/v) was used as the mobile phase at a flow rate of 1 mL/min. Two fractions (named CPT-1 and CPT-2) were separately collected as the first and second peak due to their different retention times, each with an enantiomeric excess (ee) higher than 99.8% and 99.0%, respectively. These enantiomerically "pure" fractions were used for spiking racemic CPT and determining the EMO.

Molecular modelling. The 3D structures of βCD and individual CBT enantiomers were retrieved from Cambridge Structural Database (CSD)[2] entries AGAZOX,[3] and SAZRUH and SAZSAO[4], respectively. The aliphatic nitrogen CPT was doubly protonated, thus bearing a unit positive charge, whereas the anilino group was neutral, in accord with the experimentally determined pK_a value of for 2,6-dichloroaniline.[5] The initial 3D structure of HDA-βCD was obtained from CSD entry ICUFAN (heptakis(2,3,6-tri-O-acetyl)-βCD).[6] Removal of the extra acetyl group from the O6 hydroxyl of all glucose units in this latter molecule as well as addition of the extra methyl group to both CBT enantiomers to build (*R*)- and (*S*)-CPT were accomplished by means of the editing facilities of the molecular graphics program PyMOL,[7] which was also employed for trajectory visualization and 3D figure generation. Geometry optimization of all molecules and point charge derivation were achieved by means of the AM1-BCC method,[8] as implemented in the *sqm* program[9] contained in the AMBERTools[10] distribution. The standard ff14SB force field parameter set[11] in AMBER 14[12] was used, which included in-house developed parameters for chlorine atoms attached to a phenyl ring.[13]

The four possible complexes between the two CPT enantiomers (*S* and *R*) and the two cyclodextrins were modelled upon manually docking each analyte into the CD cavity in orientations that agreed with the 1D ROESY NMR results. Each complex was then immersed in a TIP3P water box that extended 12 Å away from any solute atom (~2000 or ~2500 TIP3P water molecules for βCD and HDA-βCD, respectively) and the positive charge of CPT was neutralized by addition of one chloride ion in a random location. All hydrogens and water molecules were first reoriented in the electric field of the solute and then each whole complex was relaxed by performing 500 steps of steepest descent followed by 5000 steps of conjugate gradient energy minimization. The resulting geometry-optimized coordinate sets were used as input for unrestrained MD simulations at 300 K and a constant pressure of 1 atm using the AMBER *pmemd.cuda* engine[14] implemented in parallel on 4 GeForce Nvidia GTX980 graphics processing units (GPUs). The application of SHAKE to all bonds allowed an integration time step of 2 fs to be used. A cutoff distance of 10 Å was selected for the nonbonded interactions and the list of nonbonded pairs was updated every 25 steps. Periodic boundary

conditions were applied and electrostatic interactions were represented using the smooth particle mesh Ewald method[15] with a grid spacing of 1 Å. The coupling constants for the temperature and pressure baths were 1.0 and 0.2 ps, respectively. The water molecules and the counterion were first equilibrated around the positionally restrained solute for an initial heating period lasting 120 ps. Thereafter each whole system was allowed to evolve freely for 100 ns and coordinates from each trajectory were saved every 100 ps for analysis by means of the *cpptraj* module in AMBER.[16] A simulated annealing procedure[17] was followed every 2.5 ns to cool the system down slowly from 300 K to 273 K over a 1-ns period. Each "frozen" geometry was further optimized by carrying out an energy minimization until the root-mean-square of the Cartesian elements of the gradient was less than 0.01 kcal·mol^{-1}·Å^{-1}. We thus obtained an ensemble of 40 representative low-energy snapshots for each complex that were used to calculate the solvent-corrected interaction energies as well as their decomposition into van der Waals, coulombic, apolar, and desolvation contributions. To this end we made use of our in-house tool MM-ISMSA[18], which is so called in clear allusion to the more widely known -but much slower and cumbersome- MM-GBSA and MM-PBSA approaches. The non-electrostatic calculations involve a van der Waals term, as in molecular mechanics (MM), and the change in solvent-accessible surface area (SASA) of both binding partners brought about by complex formation. The former, which accounts for shape complementarity, is calculated with the standard AMBER 12−6 Lennard-Jones potential whereas the latter ("apolar" in the Table), representing the nonpolar part of the desolvation process, is assumed to be linearly related to a combination of the cavitation term and the van der Waals solute−solvent interactions. The solvent-screened coulombic interactions are calculated by means of an implicit solvent model (ISM) that makes use of a sigmoidal, distance-dependent dielectric function.[19]

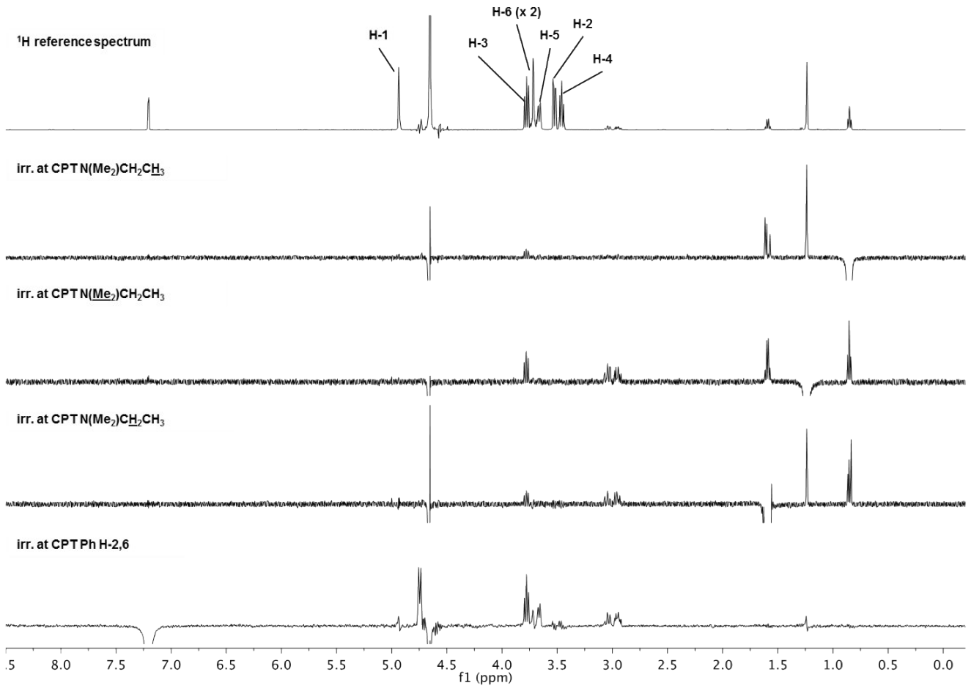

Fig. S1. Reference ^{1}H NMR spectrum of the CPT:βCD mixture (only ^{1}H signals of βCD are annotated) and 1D ROESY spectra obtained upon irradiation at the indicated CPT hydrogens.

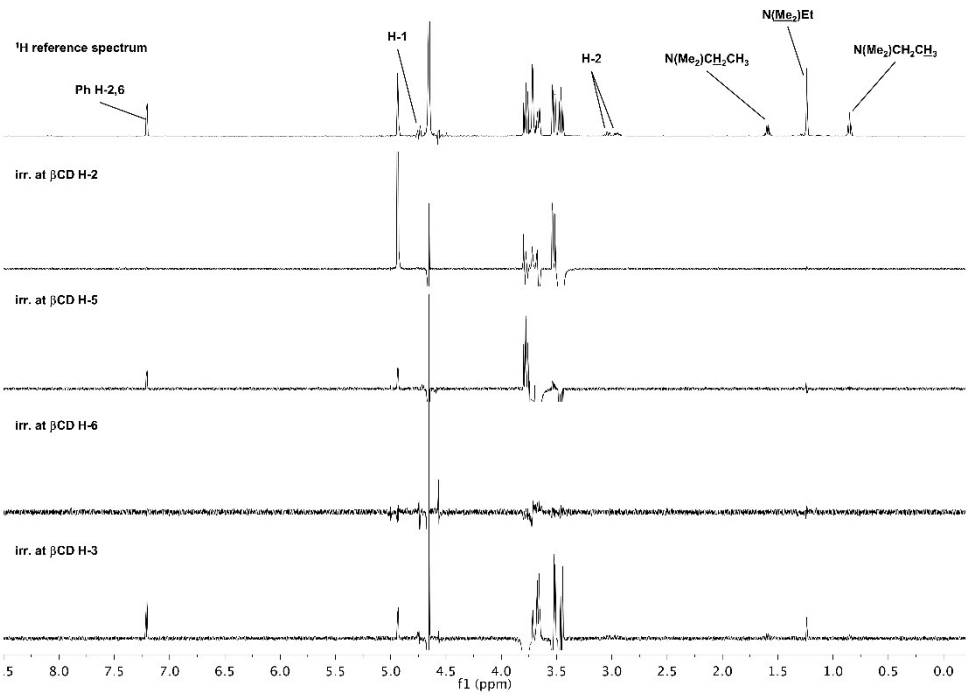

Fig. S2. Reference ^{1}H NMR spectrum of the CPT:βCD mixture (only ^{1}H signals of CPT are annotated) and 1D ROESY spectra obtained upon irradiation at the indicated βCD hydrogens.

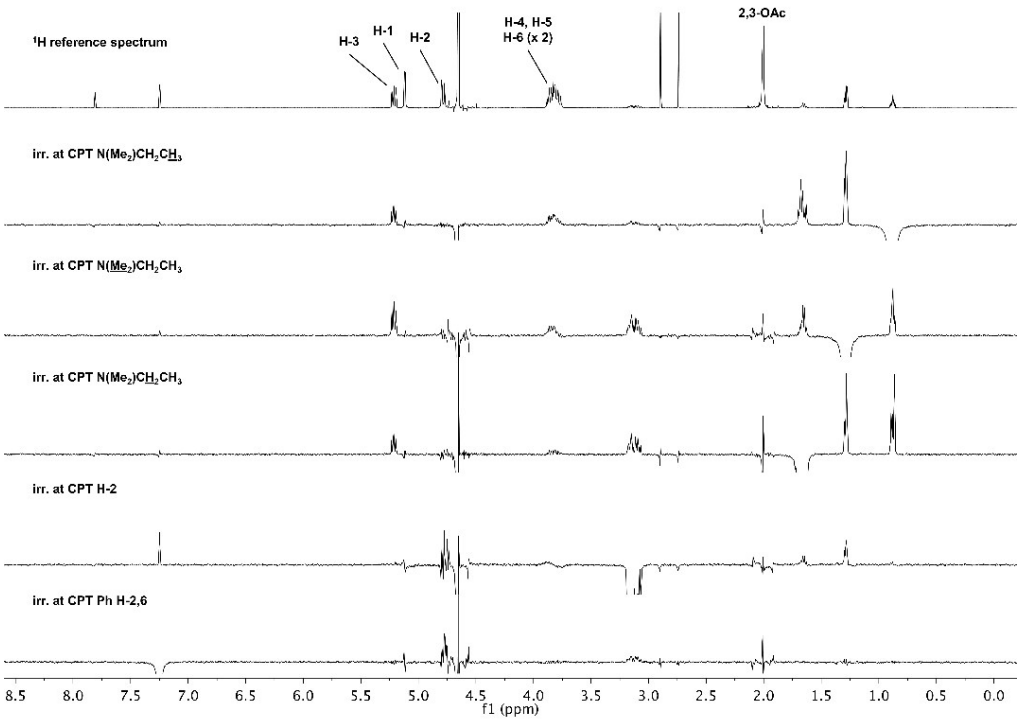

Fig. S3. Reference ^{1}H NMR spectrum of the CPT:HDA-βCD mixture (only ^{1}H signals of HDA-βCD are annotated) and 1D ROESY spectra obtained upon irradiation at the indicated CPT hydrogens.

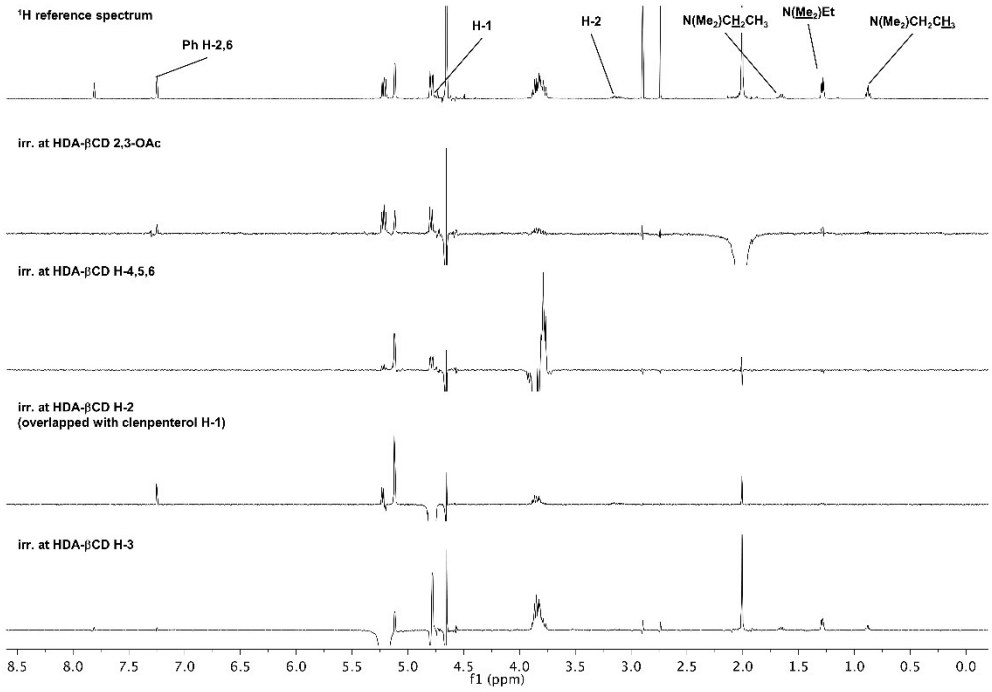

Fig. S4. Reference ^{1}H NMR spectrum of the CPT:HDA-βCD mixture (only ^{1}H signals of CPT are annotated) and 1D ROESY spectra obtained upon irradiation at the indicated HDA-βCD hydrogens.

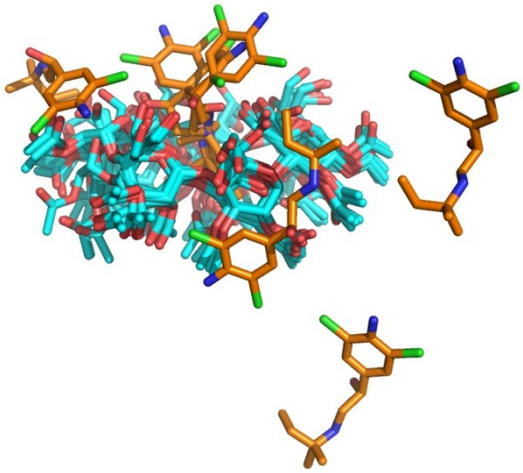

Fig. S5. Results from a test calculation, in which the orientation of CPT within HDA-βCD was the same as that reported for βCD, showing the analyte abandoning the cavity.

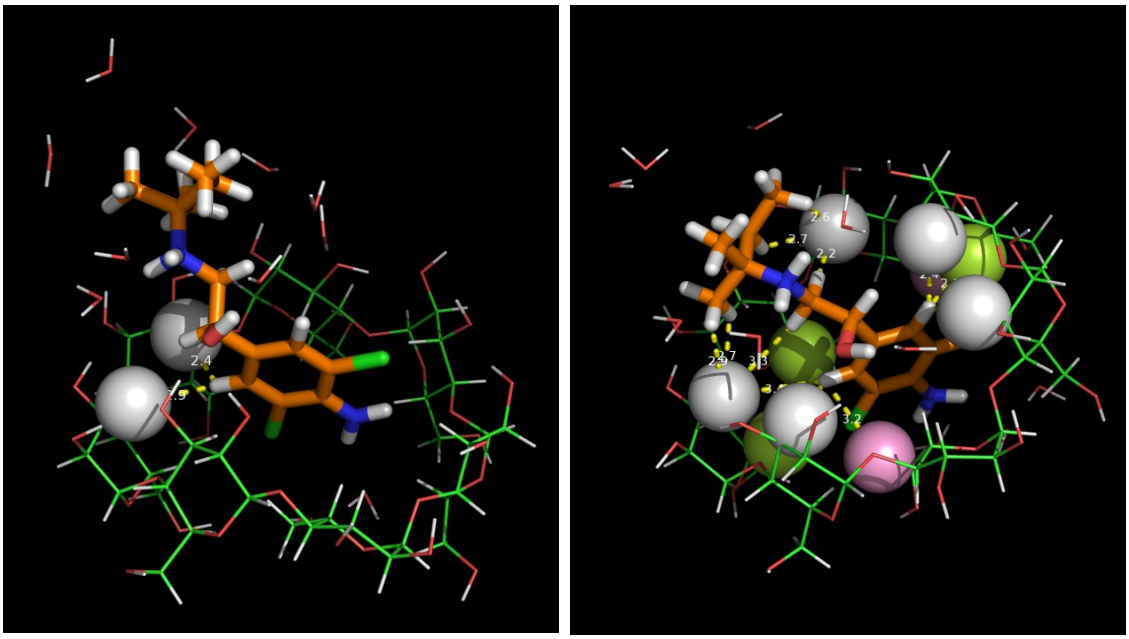

Fig. S6. Representative energy-refined snapshot from the unrestrained MD trajectories (after 100 ns of equilibration) of the modelled complexes of βCD with either (*S*)-CPT (left) or (*R*)-CPT (right) showing the interproton distances corresponding to the NOE interactions detected in the ROESY experiments.
H-3, H-5 and H-6 hydrogen atoms are displayed as spheres coloured in white, green and pink, respectively.

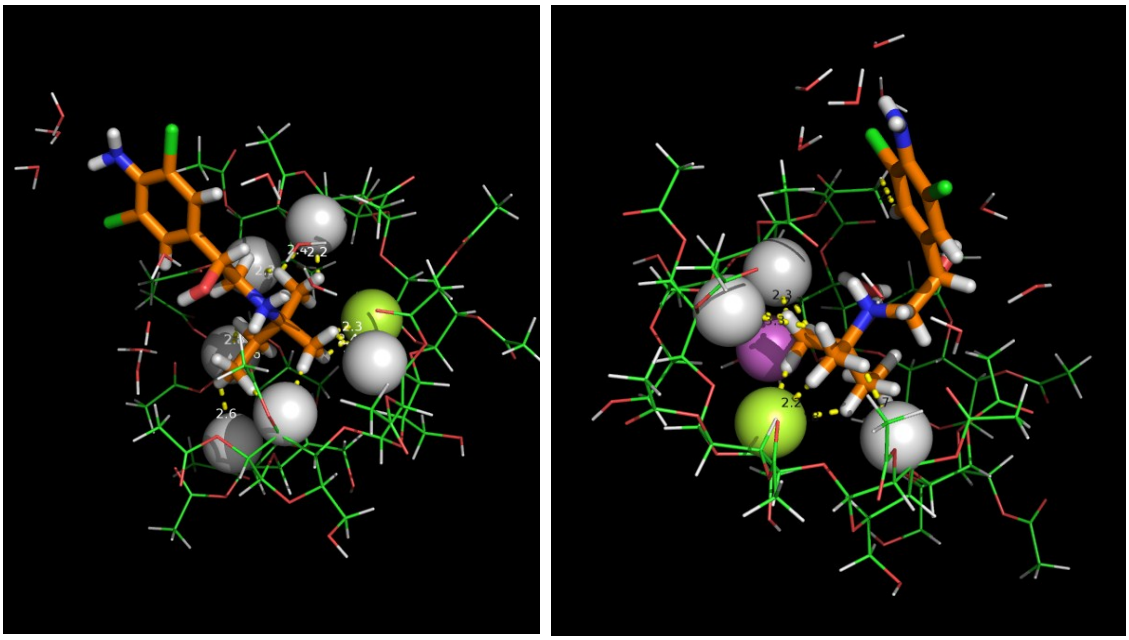

Fig. S7. Representative energy-refined snapshot from the unrestrained MD trajectories (after 100 ns of equilibration) of the modelled complexes of HDA-βCD with either (*S*)-CPT (left) or (*R*)-CPT (right) showing the interproton distances corresponding to the NOE interactions detected in the ROESY experiments.
H-3, H-5 and H-6 hydrogen atoms are displayed as spheres coloured in white, green and pink, respectively.

Supplementary Information References

1. K. Takeo, H. Mitoh and K. Uemura, *Carbohydr. Res.*, 1989, **187**, 203-221.
2. I. R. Thomas, I. J. Bruno, J. C. Cole, C. F. Macrae, E. Pidcock and P. A. Wood, *J. Appl. Crystallogr.*, 2010, **43**, 362-366.
3. J. M. Alexander, J. L. Clark, T. J. Brett and J. J. Stezowski, *Proc Natl Acad Sci U S A*, 2002, **99**, 5115-5120.
4. G.-V. Röschenthaler, E. Lork, D. V. Sevenard and W. Greb, *Z. Kristallogr. - New Cryst. Struct.*, 2005, **220**, 180-182.
5. R. A. Robinson, *J. Res. Natl. Stand. Sec. A*, 1967, **71A**, 213-218.
6. M. Añibarro, K. Gessler, I. Usón, G. M. Sheldrick, K. Harata, K. Uekama, F. Hirayama, Y. Abe and W. Saenger, *J. Am. Chem. Soc.*, 2001, **123**, 11854-11862.
7. W. L. DeLano, The PyMOL Molecular Graphics System, version 1.3, Schrödinger, LLC. (2013), http://www.pymol.org/.
8. A. Jakalian, D. B. Jack and C. I. Bayly, *J. Comput. Chem.*, 2002, **23**, 1623-1641.
9. R. C. Walker, M. F. Crowley and D. A. Case, *J. Comput. Chem.*, 2008, **29**, 1019-1031.
10. D. A. Case, T. E. Cheatham, 3rd, T. Darden, H. Gohlke, R. Luo, K. M. Merz, Jr., A. Onufriev, C. Simmerling, B. Wang and R. J. Woods, *J. Comput. Chem.*, 2005, **26**, 1668-1688.
11. J. A. Maier, C. Martinez, K. Kasavajhala, L. Wickstrom, K. E. Hauser and C. Simmerling, *J. Chem. Theory Comput.*, 2015, **11**, 3696-3713.
12. J. W. Kaus, L. T. Pierce, R. C. Walker and J. A. McCammon, *J. Chem. Theory Comput.*, 2013, **9**.
13. J. A. de la Fuente, S. Manzanaro, M. J. Martin, T. G. de Quesada, I. Reymundo, S. M. Luengo and F. Gago, *J. Med. Chem.*, 2003, **46**, 5208-5221.
14. R. Salomon-Ferrer, A. W. Götz, D. Poole, S. Le Grand and R. C. Walker, *J. Chem. Theory Comput.*, 2013, **9**, 3878-3888.
15. T. Darden, D. York and L. Pedersen, *J. Chem. Phys.*, 1993, **98**, 10089-10092.
16. D. R. Roe and T. E. Cheatham, 3rd, *J. Chem. Theory Comput.*, 2013, **9**, 3084-3095.
17. A. T. Brunger and P. D. Adams, *Acc. Chem. Res.*, 2002, **35**, 404-412.
18. J. Klett, A. Núñez-Salgado, H. G. Dos Santos, Á. Cortés-Cabrera, A. Perona, R. Gil-Redondo, D. Abia, F. Gago and A. Morreale, *J. Chem. Theory Comput.*, 2012, **8**, 3395-3408.
19. A. Morreale, R. Gil-Redondo and A. R. Ortiz, *Proteins*, 2007, **67**, 606-616.